Magnetoresistance and electronic structure of the half-metallic ferrimagnet BiCu3Mn4O12

AUTHOR(S):

Takata, K; Yamada, I; Azuma, M; Takano, M; Shimakawa, Y

CITATION:

Takata, K ...[et al]. Magnetoresistance and electronic structure of the half-metallic ferrimagnet BiCu3Mn4O12. PHYSICAL REVIEW B 2007, 76(2): 024429.

ISSUE DATE:

2007-07

URL:

http://hdl.handle.net/2433/50376

PHYSICAL REVIEW B **76**, 024429 (2007)

Magnetoresistance and electronic structure of the half-metallic ferrimagnet $BiCu_3Mn_4O_{12}$

Kazuhide Takata, Ikuya Yamada, Masaki Azuma, Mikio Takano, and Yuichi Shimakawa*
Institute for Chemical Research, Kyoto University, Uji, Kyoto 611-0011, Japan
(Received 16 March 2007; revised manuscript received 1 May 2007; published 23 July 2007)

A cubic ordered perovskite $BiCu_3Mn_4O_{12}$ has been synthesized under 6 GPa and 1000 °C. $BiCu_3Mn_4O_{12}$ is a ferrimagnet with T_C=350 K and its saturated magnetic moment is 10.5 μ_B/f.u. The material showed low-resistive metallic behavior and magnetoresistance (MR) below T_C. Its MR was observed over a wide temperature range, and the low-field MR reached −28% at 5 K. An electronic structure calculation revealed that it had a half-metallic nature and that the large MR observed under a low magnetic field was attributed to a spin-polarized tunneling or spin-dependent scattering effect at grain boundaries.

DOI: 10.1103/PhysRevB.76.024429 PACS number(s): 75.47.−m, 71.20.−b, 71.30.+h, 72.25.−b

I. INTRODUCTION

Considerable attention has been paid to the colossal magnetoresistance (CMR) effect from the viewpoints of both fundamental physics and technological application. In $R_{1-x}A_xMnO_3$ (R: rare earth ions, A: alkaline earth ions), $Tl_2Mn_2O_7$ and Sr_2FeMoO_6, for example, a half-metallic nature produces 100% spin-polarized charge carriers, which gives rise to the CMR effect. Two types of CMRs, that is, intrinsic and extrinsic CMRs, have been observed. The former is referred to as intragrain magnetoresistance (MR), in which the strong interplay between local spins and itinerant carriers plays an important role in the transport properties. This CMR usually shows its maximum near the ferromagnetic transition temperature T_C. In the manganese perovskites, a double-exchange mechanism explains the magnetotransport behavior. Near T_C, thermally fluctuated local spins are forced to align by an external field, leading to drastically reduced resistivity. The latter is intergrain MR, which is attributed to spin-polarized tunneling through a very thin insulating barrier or spin-dependent scattering at grain boundaries in polycrystalline samples. This MR often occurs under a low magnetic field over a wide temperature range below T_C. Since large MR at a low applied field above room temperature (RT) is highly desirable from the viewpoint of practical application, the extrinsic MR effects of polycrystalline manganese perovskites and Sr_2FeMoO_6 have been extensively studied.

Another example of intergrain MR has recently been found in a complex perovskite-structure oxide, $CaCu_3Mn_4O_{12}$. This compound is a ferrimagnet (T_C=355 K) and a polycrystalline sample showed a good low-field response below T_C, with a value as large as −12% at 0.05 T and 20 K.[1] A band-structure calculation by Weht and Pickett revealed that this material has a spin-asymmetric gap.[2] Thermally induced electrons are doped into up-spin Mn e_g levels, giving rise to spin-polarized semiconducting behavior with resistivity of about 1.8×10^3 Ω cm at RT.

$CaCu_3Mn_4O_{12}$ was extensively studied in the 1970s because it has a high ferrimagnetic transition temperature.[3,4] This material crystallizes in an A-site ordered perovskite structure, that is, Jahn-Teller Cu^{2+} and Ca^{2+} ions are ordered in a $2a\times2a\times2a$ cubic unit cell. The ferrimagnetic interaction originates from antiferromagnetic coupling between Cu^{2+} $\left(d^9, S=\frac{1}{2}\right)$ and Mn^{4+} $\left(d^3, S=\frac{3}{2}\right)$ spins. Although the ideal ferrimagnetic ordering of Cu^{2+} and Mn^{4+} spins produces $9\mu_B$/f.u., partial substitution of Mn for Cu often reduces the magnetization.[5] Ca^{2+} ions at the A-site can be replaced by R^{3+} ions, and the substitution produces electrons into Mn at the B site. $LaCu_3Mn_4O_{12}$ is an example of this substitution and it shows low-resistive metallic behavior. Similar to $CaCu_3Mn_4O_{12}$, the reported $LaCu_3Mn_4O_{12}$ compound had a Mn-rich composition like $LaCu_{2.7}Mn_{4.3}O_{11.8}$, which was confirmed by structural study using neutron powder diffraction.[6] Thus, the saturated magnetization was about $8.4\mu_B$/f.u., which was much smaller than the value of $10\mu_B$/f.u. expected from the stoichiometric composition. This antisite substitution decreases the ferrimagnetic magnetization.

In this study, we succeeded in preparing a complex oxide $BiCu_3Mn_4O_{12}$ by means of high-pressure synthesis. In contrast to $CaCu_3Mn_4O_{12}$ and $LaCu_3Mn_4O_{12}$, the obtained material showed no Mn substitution for Cu in the crystal structure. $BiCu_3Mn_4O_{12}$ showed a large magnetic moment as expected from the ideal composition below the ferrimagnetic Curie temperature at 350 K. The half-metallic nature revealed by a band-structure calculation causes large MR at a low magnetic field.

II. EXPERIMENTS

A bulk sample of $BiCu_3Mn_4O_{12}$ was prepared under high-temperature and high-pressure conditions. MnO_2 raw material was prepared by firing MnOOH powder at 300 °C in air. A mixture of $\frac{1}{2}Bi_2O_3+3CuO+\frac{1}{2}Mn_2O_3+3MnO_2$ was charged into a gold capsule and treated at 6 GPa and 1000 °C for 30 min in a cubic-anvil-type high-pressure apparatus. The sample was then quenched to room temperature before the pressure was released. The crystal structure of the obtained sample was analyzed by synchrotron x-ray powder diffraction (XRD) taken with the large Debye-Scherrer camera[7] installed at BL02B2 of SPring-8 with λ =0.421 53 Å. The RIETAN-2000 program[8] was used for the structure refinement. Magnetic properties were measured with a superconducting quantum interference device magnetometer (Quantum Design MPMS XL) for the temperature range from 400 to 5 K. Transport properties were measured by a four-probe method. The electronic structure of $BiCu_3Mn_4O_{12}$ was calculated by the linearized augmented

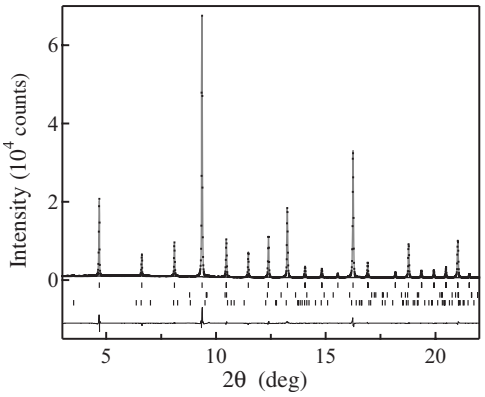

FIG. 1. Synchrotron x-ray powder diffraction pattern (dots) and the calculated (solid line) profile of Rietveld refinement for $BiCu_3Mn_4O_{12}$ ($\lambda = 0.421\,53$ Å). Differences between the observed and the calculated intensities are shown at the bottom. Thick marks correspond to the Bragg angle positions of $BiCu_3Mn_4O_{12}$ (top), $Bi_2(CO_3)O_2$ (second), and CuO (third).

plane-wave (LAPW) method with the WIEN2k code. The experimental lattice constant and the atomic positional parameters obtained by the structural refinement were used for the calculation. LAPW sphere radii were 1.60, 2.00, 2.00, and 1.60 for Bi, Cu, Mn, and O, respectively. Self-consistency was carried out on 60 k-point meshes in the irreducible Brillouin zone. The generalized gradient approximation exchange-correlation function was used.

III. RESULTS AND DISCUSSION

A. Crystal structure

$BiCu_3Mn_4O_{12}$ obtained by the high-pressure synthesis was well-crystallized black powder and was almost single phase. Figure 1 shows the synchrotron XRD pattern of $BiCu_3Mn_4O_{12}$ and the results of fitting by Rietveld analysis. Small amounts of impurity phases, 0.10 wt % $Bi_2(CO_3)O_2$ and 0.79 wt % CuO, were included in the refinement. The XRD pattern is characteristic of a cubic perovskite with superstructure reflections due to the 1:3 ordering of Bi and Cu ions. All diffraction peaks are indexed with a $2a \times 2a \times 2a$ cubic cell of $Im\bar{3}$ symmetry, which is the same as that of $CaCu_3Mn_4O_{12}$. In the structure refinement, Bi, Cu, Mn, and O atoms were placed at $2a$ (0, 0, 0), $6b$ (0, $\frac{1}{2}$, $\frac{1}{2}$), $8c$ ($\frac{1}{4}$, $\frac{1}{4}$, $\frac{1}{4}$), and $24g$ (x,y,0) sites, respectively. No apparent vacancy was observed at any site, so each occupation factor g was fixed at 1. Although XRD is insensitive to the substitution of Mn for Cu as seen in $LaCu_{3-x}Mn_{4+x}O_{12-\delta}$, such a possibility can be ruled out for our sample. Since the amount of impurity phases in the resultant sample is very small, cation stoichiometry should be maintained during the confined condition of the high-pressure synthesis. The result of magnetic measurement discussed in the next section also strongly supports the absence of cation nonstoichiometry. A reasonable fit, $R_{wp}=3.46$, $S=1.16$, and $R_I=1.81\%$, was obtained with this model. The refined unit-cell parameter was 7.305 16(6) Å, and the refined structural parameters are summarized in Table I. The structure model determined by the refinement is also shown in Fig. 2. At the A site, the Bi ions are isotropically coordinated to 12 oxygen ions with Bi-O bond length of 2.577(2) Å, while the Cu ions make an almost square coordination to oxygen due to significantly tilted MnO_6 octahedra. The Mn-O-Mn and Cu-O-Mn angles are 142.47(14)° and 108.48(6)°, respectively. The refined Mn-O distance is 1.9288(6) Å, which is longer than 1.915(1) Å observed in $CaCu_3Mn_4O_{12}$. Since the chemical composition of $BiCu_3Mn_4O_{12}$ induces mixed valence for the Mn ion such as $Bi^{3+}Cu_3{}^{2+}Mn_4{}^{3.75+}O_{12}{}^{2-}$, the result is consistent with the incorporation of larger Mn^{3+} ions in the Mn^{4+} sublattice. A bond valence sum[8] calculation from the refined structural parameters also gave 3.73+ for the B-site Mn ion, which is close to the nominal valence of 3.75+. The result obtained from the structure analysis strongly indicates the $(BiCu_3)$ A-site ordering for the perovskite structure and the incorporation of Mn^{3+} in the Mn^{4+} sublattice.

TABLE I. Refined structural parameters of $BiCu_3Mn_4O_{12}$ from Rietveld analysis of synchrotron XRD data. Numbers in parentheses are standard deviations of the last significant digit. Space group: $Im\bar{3}$. $a=7.305\,16(6)$ Å, $R_{wp}=3.46\%$, $R_p=2.42\%$, $R_I=1.81\%$, $R_F=0.57\%$, and $Re=2.98\%$.

Atom	Site	g	x	y	z	B (Å^2)
Bi	$2a$	1	0	0	0	0.97(1)
Cu	$6b$	1	0	$\frac{1}{2}$	$\frac{1}{2}$	0.58(1)
Mn	$8c$	1	$\frac{1}{4}$	$\frac{1}{4}$	$\frac{1}{4}$	0.23(1)
O	$24g$	1	0.301 8(3)	0.182 7(3)	0	0.54(5)

B. Magnetic properties and magnetoresistance

$BiCu_3Mn_4O_{12}$ shows spontaneous magnetization below 350 K. The M (magnetization)-H (applied magnetic field)

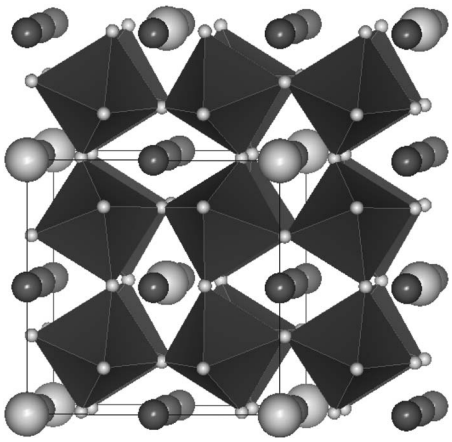

FIG. 2. Crystal structure of $BiCu_3Mn_4O_{12}$. The octahedra correspond to MnO_6. Bi and Cu ions drawn with large white and small dark gray spheres, respectively, are ordered at the A site in the perovskite structure.

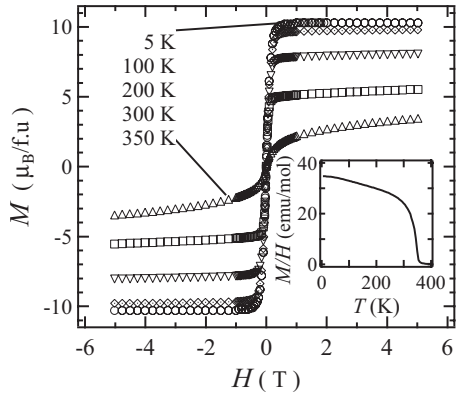

FIG. 3. M-H curves of $BiCu_3Mn_4O_{12}$ at various temperatures. The inset shows the temperature dependence of M/H measured at 0.1 T from 400 to 5 K.

behaviors at various temperatures and the temperature dependence of the magnetic susceptibility are shown in Fig. 3. The observed saturated magnetic moment (M_S) at 5 K is about $10.5\mu_B$/f.u. If we assume antiparallel alignment between Mn and Cu spins for the composition of $BiCu_3Mn^{3+}Mn_3{}^{4+}O_{12}$ (Cu^{2+}, $S=\frac{1}{2}$; Mn^{3+}, $S=2$; Mn^{4+}, $S=\frac{3}{2}$), then the saturated ferrimagnetic moment should be $10\mu_B$/f.u., which is quite close to the observed value. This is in sharp contrast to $LaCu_3Mn_4O_{12}$, for which the reported saturated magnetic moment, $8.4\mu_B$/f.u., is smaller than the expected value ($10\mu_B$/f.u.). Although Sunchez-Benites *et al.* proposed a spin canting model of the magnetic moments at the B-site ions in $CaCu_{2.5}Mn_{4.5}O_{12}$,[9] we see no trace of such canting moments in our sample. The observed magnetization shows the saturation ($10.5\mu_B$/f.u.) at about 0.5 T and no increase at higher magnetic fields. We therefore conclude that the large magnetic moment observed in $BiCu_3Mn_4O_{12}$ is a result of ferrimagnetic ordering of A-site Cu and B-site Mn spins and there are no indications of a cation substitution or spin canting effect.

The resistivity of $BiCu_3Mn_4O_{12}$ is as low as 10^{-3} Ω cm and the material clearly shows low-field magnetoresistance below the ferrimagnetic transition temperature. Figure 4 shows the MR ratio, defined as $MR(H)=[R(H)-R(0)]/R(0)$, under magnetic fields at various temperatures. At 5 K, the low-field MR below 1 T is as large as −28%, and

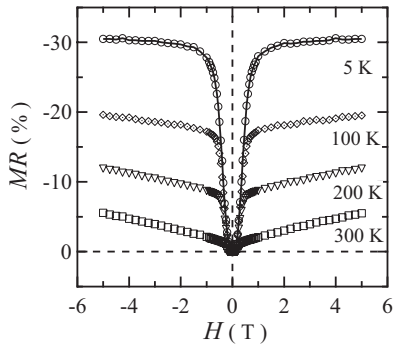

FIG. 4. MR ratios of $BiCu_3Mn_4O_{12}$ at various temperatures.

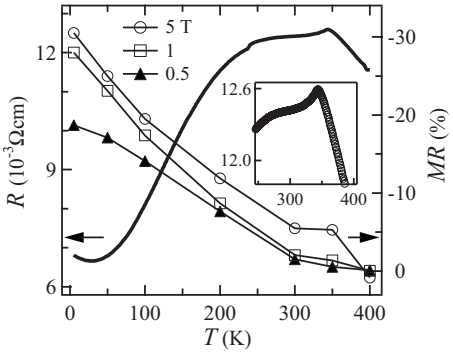

FIG. 5. Temperature dependence of resistivity at 0 T and MR ratio at 0.5 T (triangles), 1 T (squares), and 5 T (circles).

MR reaches −31% at 5 T. The changes in MR are quite consistent with the changes in magnetization. At low applied fields of less than 1 T, resistivity significantly decreases with increasing magnetization, and it saturates in accordance with the saturation in magnetization. Since the change in magnetization in a polycrystalline sample below T_C corresponds to the change in alignment of magnetic domains, the observed large MR under low magnetic field should be a result of a grain- or domain-boundary effect. It should also be noted that MR is still significant at room temperature. The observed MR values are about −2% and about −6% at 1 and 5 T, respectively.

The temperature dependence of the resistivity of $BiCu_3Mn_4O_{12}$ is illustrated in Fig. 5. As mentioned above, the observed resistivity ρ ($T=300$ K, $H=0$) of 12 mΩ cm is considerably lower than that reported for the compound $CaCu_3Mn_4O_{12}$. It is worth mentioning that the resistivity at $H=0$ displays a metallic behavior below T_C and semiconducting behavior above T_C. The distinct change in the temperature dependence of the resistivity at T_C implies that the transport properties of $BiCu_3Mn_4O_{12}$ are strongly affected by the magnetic properties. In the ferrimagnetic state below T_C, the sample changes to a metallic state and the resistivity decreases. It should also be pointed out that the MR is observed over a wide temperature range below T_C, and the value increases with decreasing temperature. This is quite similar to that observed in Sr_2FeMoO_6, in which low-field MR is attributed to the grain- or domain-boundary effect in polycrystalline samples.

C. Electronic structure

The electronic structure of $BiCu_3Mn_4O_{12}$ was calculated for the ferrimagnetically ordered ground state as indicated by the magnetic measurement. The calculated magnetic moments inside the muffin tin spheres are 2.66 and $-0.44\mu_B$/f.u. for Mn and Cu ions, respectively. The reduction from the ideal value results from hybridization with the O $2p$ state. The total magnetic moment is $10.00\mu_B$/f.u., which agrees well with the experimentally observed saturated magnetic moment and the moment expected from the ferrimagnetic ordering of Mn and Cu spins for the composition of $BiCu_3Mn^{3+}Mn_3{}^{4+}O_{12}$.

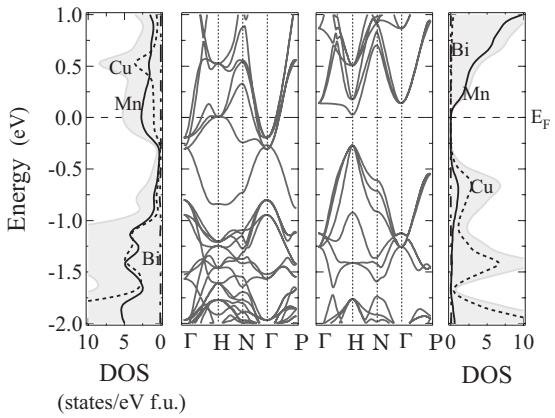

FIG. 6. Electronic band structure and density of states (DOS) of $BiCu_3Mn_4O_{12}$ for up spins (left panels) and down spins (right panels). Calculation was performed for the ferrimagnetically ordered ground state. Total densities of states (shaded region) and partial density of states for Mn (solid line), Cu (dashed line), and Bi (dashed-and-dotted line) are shown in the DOS figures.

The calculated band structures and the corresponding density of states (DOS) for up and down spins are shown in Fig. 6. In sharp contrast to the spin-asymmetric insulating band structure of $CaCu_3Mn_4O_{12}$, up-spin conduction bands cross the Fermi level. These bands mainly consist of Mn e_g states. This is consistent with the ionic picture, in which the Bi^{3+} incorporation induces mixed valence for the Mn ion such as $Mn^{3.75+}$. It should be noted that the band structure for $BiCu_3Mn_4O_{12}$ is also spin asymmetric, and the half-metallic nature produces spin-polarized conduction electrons in this material. The down-spin bands at the valence band maximum, on the other hand, have a strong Cu $3d$ character hybridized with O $2p$. The calculated band structure of our $BiCu_3Mn_4O_{12}$ is very similar to that reported for $LaCu_3Mn_4O_{12}$.[10] The bands originating from Bi ions appear to play a less important role in the metallic conductivity and magnetoresistanace. Although Liu *et al.* discussed an intrinsic magnetoresistance mechanism in $LaCu_3Mn_4O_{12}$, we believe that the observed low-field MR in $BiCu_3Mn_4O_{12}$ is extrinsic effect of polycrystalline samples.

IV. CONCLUSION

A half-metallic ferrimagnet $BiCu_3Mn_4O_{12}$ was synthesized at 6 GPa and 1000 °C. The mixed valence in Mn (3.75+) and ferrimagnetic ordering of *A*-site Cu and *B*-site Mn spins lead to the half-metallic nature and produce spin-polarized conduction carriers. The compound shows large magnetoresistance under low magnetic fields, which is attributed to a spin-polarized tunneling or spin-dependent scattering effect at grain or domain boundaries. The relatively high ferrimagnetic transition temperature (T_C=350 K) of this material could be a great advantage for possible magnetoresistive applications.

ACKNOWLEDGMENTS

We thank Y. Ikeda for providing us with the MnOOH raw material. We also thank M. Tsujimoto, H. Kurata, S. Isoda, and A. Masuno for their help in the electronic structure calculations and for fruitful discussion. This work was partly supported by the Grants-in-Aid for Scientific Research (No. 17105002, No. 1738014, and No. 18350097) from the Ministry of Education, Culture, Sports, Science and Technology (MEXT) of Japan. The synchrotron radiation experiments were performed at SPring-8 with the approval of the Japan Synchrotron Radiation Research Institute.

*Corresponding author; shimak@scl.kyoto-u.ac.jp

[1] Z. Zeng, M. Greenblatt, M. A. Subramanian, and M. Croft, Phys. Rev. Lett. **82**, 3164 (1999).
[2] R. Weht and W. E. Pickett, Phys. Rev. B **65**, 014415 (2001).
[3] J. Chenavas, J. C. Joubert, M Marezio, and B. Bochu, J. Solid State Chem. **14**, 25 (1975).
[4] B. Bochu, J. C. Joubert, A. Collomb, B. Ferrand, and D. Samaras, J. Magn. Magn. Mater. **15**, 1319 (1980).
[5] Z. Zeng, M. Greenblatt, J. E. Sunstrom IV, M. Croft, and S. Khalid, J. Solid State Chem. **147**, 185 (1999).
[6] J. A. Alonso, J. Sanchez-Benitez, A. De Andres, M. J. Martinez-Lope, M. T. Casais, and J. L. Martinez, Appl. Phys. Lett. **83**, 2623 (2003).
[7] E. Nishibori, M. Takata, K. Kato, M. Sakata, Y. Kubota, S. Aoyagi, Y. Kuroiawa, M. Yamakata, and N. Ikeda, Nucl. Instrum. Methods Phys. Res. A **467-568**, 1045 (2001).
[8] F. Izumi and T. Ikeda, Mater. Sci. Forum **321-323**, 198 (2000).
[9] J. Sanchez-Benitez, J. A. Alonso, M. J. Martinez-Lope, M. T. Casais, J. L. Martinez, A. De Andres, and M. T. Fernandez-Diaz, Chem. Mater. **15**, 2193 (2003).
[10] X. J. Liu, H. P. Xiang, P. Cai, X. F. Hao, and Z. J. Meng, J. Mater. Chem. **16**, 4243 (2006).